Numerical Study of The Generalised Serre-Green-Naghdi Model

Contents

1. Introduction

The simulation of gravity waves of fluids plays a pivotal role in the modelling of important and interesting physical phenomena such as tsunamis [], storm surges [] and riverine flooding[]. Such phenomena are routinely shallow water phenomena, where the typical water depth H is much smaller than the typical wave length λ, such that shallowness parameter $\sigma = H/\lambda \ll 1$.

A variety of equations have been developed for waves in this shallow water regime []. These equations are usually characterised by the powers of σ retained in their approximation to the full Euler equations, as well as the allowable size of the non-linearity parameter $\eta = A/H$ where A is the typical wave amplitude. Important members of this family of shallow water wave models are; the shallow water wave equations (SWWE) which retains only the first power of σ [1] and are fully non-linear so that $\eta = O(1)$ and the Serre-Green-Naghdi (SGN) equations which retain up to the third powers of σ and are also fully non-linear [1].

There are equations corresponding to any power of σ retained, with each power of σ allowing for more accurate modelling of waves as the shallowness restriction is relaxed and σ increases. However, as more powers of σ are retained higher order derivative terms appear in the equations, which can be difficult to treat analytically and numerically. Hence, the focus on lower order σ approximations. Particular attention has been on the dispersion relationship of these equations, which relates the angular frequency ω to the wave number k for solutions of the linearised equations. This focus is due to the utility of the dispersion relationship in determining the behaviour of the corresponding non-linear equations [].

Recently, [2] demonstrated a family of equations that improve the dispersion relationship of the SGN equations with only a minor increase in complexity, the so called improved SGN (iSGN). The iSGN family of equations was then expanded to the generalised SGN equations (gSGN), a family of equations that includes the

SWWE, the SGN equations, the iSGN family and the regularised shallow water wave equations (rSWWE) [3]. The rSWWE are regularised in the sense that the shocks observed in solutions of the SWWE become regularised (smoothed) shocks that are no longer discontinuous.

This family of equations contains many members that are of current interest to the numerical wave modelling community []. Thus a numerical method that can solve these equations allows for a single point of comparison between the numerical solutions of many different equations of interest. We propose a method to solve the gSGN that relies on generalising the methods for the SGN equations presented in [].

This numerical method is then validated using analytic solutions of the SGN and the SWWE, demonstrating its convergence rate and conservation properties. Additionally, we also make use of Forced solutions to validate that all terms in the gSGN are being accurately approximated to the correct order of accuracy. Forced solutions are necessary to validate the numerical method for the more general members of this family of equations, outside the well tested members.

Finally, using the well validated numerical method we perform a numerical investigation into the behaviour of this family of equations for a smoothed dambreak problem. This problem is of particular interest firstly, because this problem requires that the numerical method is robust in the presence of steep gradients. Secondly, the solution of steep smoothed dam-break problems requires the resolution of very high wave-number waves allowing us to see the full effect of the changes in the numerical solutions between different members of the family. Thirdly, for the rSWWE we will be able to demonstrate the transition along the rSWWE family, as it approaches the standard SWWE.

Background

- Why
  - Dispersive wave equations to model phenomena
  - New regularisation techniques to improve dispersive properties without requiring additional higher derivative terms (Denys - improved dispersion paper)
  - Regularisation techniques to produce regularised shock waves - (other denys paper)
  - The equations capture this new areas whilst possessing conservation law forms
  - Such generalised equations will allow us to gain insight into heuristic processes such as switching off dispersion/ regularisation

Contributions

- Numerical illustrations, but no concrete methods with validation in literature
- Robust numerical method
- Numerical study of effect of beta values, in particular for various interesting classes

2. Generalised Serre-Green-Naghdi Equations

The gSGN equations derived by Clamond and Dutykh [3] generalise the SGN equations that describe a depth averaged approximation to the Euler equations [] where h is the height of the free-surface of the water, u is the depth averaged velocity and g is the acceleration due to gravity. The gSGN equations accomplish this by introducing two free parameters β_1 and β_2, that when fixed result in a particular member of this family of equations. The gSGN equations are particularly desirable due to their generalisation of the SGN equations for conservation of mass, momentum and energy like so:

$$\frac{\partial h}{\partial t} + \frac{\partial (hu)}{\partial x} = 0 \tag{1a}$$

$$\frac{\partial (hu)}{\partial t} + \frac{\partial}{\partial x}\left(hu^2 + \frac{1}{2}gh^2 + \frac{1}{3}h^2\Gamma \right) = 0 \tag{1b}$$

$$\begin{aligned} &\frac{\partial}{\partial t}\left[\frac{1}{2}hu^2 + \frac{1}{4}\left(\frac{2}{3}+\beta_1\right)h^3\frac{\partial u}{\partial x}\frac{\partial u}{\partial x} + \frac{1}{2}gh^2\left(1+\frac{1}{2}\beta_2\frac{\partial h}{\partial x}\frac{\partial h}{\partial x}\right)\right] \\ &\quad + \frac{\partial}{\partial x}\left[hu\left(\frac{1}{2}u^2 + \frac{1}{4}\left(\frac{2}{3}+\beta_1\right)h^2\frac{\partial u}{\partial x}\frac{\partial u}{\partial x} + gh\left(1+\frac{1}{4}\beta_2\frac{\partial h}{\partial x}\frac{\partial h}{\partial x}\right) + \frac{1}{3}h\Gamma\right) + \frac{1}{2}\beta_2 gh^3\frac{\partial h}{\partial x}\frac{\partial u}{\partial x}\right] = 0 \end{aligned} \tag{1c}$$

Resulting Equations	β_1	β_2
SGN Equations	0	0
SWWE	$-\frac{2}{3}$	0
rSWWE Family	free variable	$\beta_1 + \frac{2}{3}$
iSGN Family	free variable	β_1
SGN to SWWE Family	$-\frac{2}{3} \leq \beta_1 \leq 0$	0

Table 1: Important members and families of equations of the gSGN in terms of the associated β values. Here free variable, indicates that any chosen value of β_1 is a member of the family, provided that β_2 is defined in terms of β_1 in the corresponding way.

where

$$\Gamma = \frac{3}{2}\left(\frac{2}{3}+\beta_1\right) h\left[\frac{\partial u}{\partial x}\frac{\partial u}{\partial x} - \frac{\partial^2 u}{\partial x \partial t} - u\frac{\partial^2 u}{\partial x^2}\right] - \frac{3}{2}\beta_2 g\left[h\frac{\partial^2 h}{\partial x^2} + \frac{1}{2}\frac{\partial h}{\partial x}\frac{\partial h}{\partial x}\right] \tag{1d}$$

I have summarised the important members (pairs of β values) and families (groups of pairs of β values) in Table 1. Equations (1a) - (1c) hold for all β values provided the solutions are sufficiently smooth. However, for particular β values, for example those corresponding to the SWWE, it is possible to obtain non-smooth solutions for any pair of these equations that no longer satisfy all three equations simultaneously []. This particular issue with the SWWE, is one of impetuses for regularising them in the rSWWE family.

2.1. Dispersion Relation of Linearised gSGN

Linearising the gSGN (1) for small waves on a mean flow depth h_0 and mean flow velocity u_0 and seeking travelling wave solutions of the form $\exp(i(kx-\omega t))$ as was done by [] we obtain the dispersion relation

$$\omega^{\pm} = u_0 k \pm k\sqrt{gh_0}\sqrt{\frac{\beta_2 h_0^2 k^2 + 2}{\left(\frac{2}{3}+\beta_1\right)h_0^2 k^2 + 2}}. \tag{2}$$

This dispersion relation provides the angular freqeuncy ω of travelling wave solutions of the linearised gSGN equations for wave with wavenumber k. This dispersion relation (2) is equivalent to the dispersion relation derived by [3] when $u_0 = 0$.

From the dispersion relation (2), the phase speed v_p and the group speed v_g can be derived as follows

$$v_p^{\pm} = \frac{\omega^{\pm}}{k} = u_0 \pm \sqrt{gh_0}\sqrt{\frac{\beta_2 h_0^2 k^2 + 2}{\left(\left(\frac{2}{3}+\beta_1\right)h_0^2 k^2 + 2\right)}}, \tag{3a}$$

$$v_g^{\pm} = \frac{\partial \omega^{\pm}}{\partial k} = u_0 \pm \sqrt{gh_0}\sqrt{\frac{\beta_2 h_0^2 k^2 + 2}{\left(\left(\frac{2}{3}+\beta_1\right)h_0^2 k^2 + 2\right)}}\left[1 + \frac{\beta_2 - \left(\beta_1 + \frac{2}{3}\right)}{\left(\frac{1}{2}\beta_2 h_0^2 k^2 + 1\right)\left(\left(\frac{1}{3}+\beta_1\right)h_0^2 k^2 + 1\right)}\right]. \tag{3b}$$

For the appropriate choices of β values we recover the dispersion relationship and thus the phase and group speeds of the SGN [] and the SWWE [].

2.1.1. Wave Speed Bounds

[] made use of bounds on the phase speeds for the SGN, to apply approximate Riemann solvers such as those of [] to solve the SGN. Thus, if the gSGN can also be shown to have bounds on the phase speeds then such techniques can be applied to the gSGN. Thus we want to demonstrate which β values force the phase speeds of the gSGN to be bounded.

The proof of this can be seen by observing that when $\beta_1 \geq -\frac{2}{3}$, $\beta_2 \geq 0$ and $h_0 k \geq 0$ we have that

$$f_1(h_0 k) = \frac{\beta_2 (h_0 k)^2 + 2}{\left(\left(\frac{2}{3}+\beta_1\right)(h_0 k)^2 + 2\right)},$$

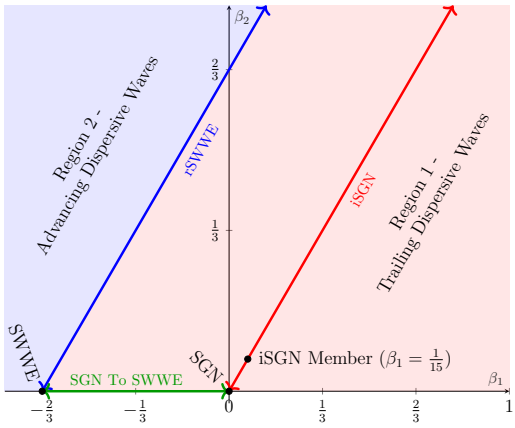

Figure 1: Plot phase speed regions of β_1 and β_2 showing important families of equations and particular members of these families.

is a monotone function over $h_0 k$. This can be seen by reformulating and taking the derivative with respect to $h_0 k$, to obtain that

$$\frac{\partial\left(f_1(h_0k)\right)}{\partial\left(h_0k\right)} = \left[\frac{\beta_2}{\beta_1+\frac{2}{3}} - 1\right] \frac{\frac{4}{\beta_1+\frac{2}{3}}\left(h_0k\right)}{\left(\frac{4}{\beta_1+\frac{2}{3}} + \left(h_0k\right)^2\right)^2}.$$

The derivative is greater than 0 and thus monotone non-increasing if $\beta_2 \leq \frac{2}{3} + \beta_1$ and less than 0 and thus monotone non-decreasing if $\beta_2 \leq \frac{2}{3} + \beta_1$ given the initial assumptions. It can therefore be seen that under the initial assumptions that v_p^+ is monotone non-decreasing and v_p^- is monotone non-increasing when $\beta_2 \leq \frac{2}{3} + \beta_1$ and v_p^- is monotone non-increasing and v_p^- is monotone non-decreasing when $\beta_2 \geq \frac{2}{3} + \beta_1$.

In addition to the monotonicity of $v_p^\pm$ we have that as $k \to 0$ then $v_p^\pm \to u_0 \pm \sqrt{gh_0}$ whilst as $k \to \infty$ then $v_p^\pm \to u_0 \pm \sqrt{gh_0}\sqrt{\frac{\beta_2}{\frac{2}{3}+\beta_1}}$. Together these results demonstrate that the phase speeds are bounded for all β values provided that $\beta_1 = -\frac{2}{3}$ only when $\beta_2 = 0$, otherwise the $k \to \infty$ limit, is no longer bounded.

The extra care taken to identify when checking the monotonicty of $v_p^\pm$, can be used to demonstrate that when $\beta_2 \leq \frac{2}{3} + \beta_1$ then the following chain of inequalities holds

$$u_0 - \sqrt{gh_0} \leq v_p^- \leq u_0 - \sqrt{gh_0}\sqrt{\frac{\beta_2}{\frac{2}{3}+\beta_1}} \leq u_0 \leq u_0 + \sqrt{gh_0}\sqrt{\frac{\beta_2}{\frac{2}{3}+\beta_1}} \leq v_p^+ \leq u_0 + \sqrt{gh_0}. \tag{4}$$

We designate this region of β values, as Region 1, it is characterised by either lack of dispersion when $\beta_2 = \frac{2}{3} + \beta_1$ or trailing discursive waves when $\beta_2 < \frac{2}{3} + \beta_1$. Region 1 includes the SWWE, the SGN, the rSWWE family, and the iSGN family, it is also the behaviour of the dispersion of actual water waves [].

When $\beta_2 > \frac{2}{3} + \beta_1$ the inequality chain becomes

$$u_0 - \sqrt{gh_0}\sqrt{\frac{\beta_2}{\frac{2}{3}+\beta_1}} \leq v_p^- \leq u_0 - \sqrt{gh_0} \leq u_0 \leq u_0 + \sqrt{gh_0} \leq v_p^+ \leq u_0 + \sqrt{gh_0}\sqrt{\frac{\beta_2}{\frac{2}{3}+\beta_1}} \tag{5}$$

We call this Region 2, and it is characterised by advancing dispersive waves. Advancing dispersive waves are not observed for water waves, and thus none of our equations or family of equations of interest lie in this region. We will therefore, be restricting our study to the Region 1 in this paper.

The location of important members and families of equations in terms of β values is summarised in Figure 1.

2.2. Alternative Conservative Form of the gSGN

Clamond and Dutykh [3] demonstrate how to rearrange (1b) for the rSWWE, in an analagous way to the reformulations of SGN demonstrated by []. The purpose of doing this is to remove the mixed spatial-temporal

derivative, which is difficult to treat numerically. The reformulation works analogously for the gSGN equations as well, and so we can obtain an equivalent formulation of (1b) which becomes

$$\frac{\partial G}{\partial t} + \frac{\partial}{\partial x}\left(uG + \frac{gh^2}{2} - \left(\frac{2}{3} + \beta_1\right) h^3 \frac{\partial u}{\partial x}\frac{\partial u}{\partial x} - \frac{1}{2}\beta_2 g h^2 \left[h\frac{\partial^2 h}{\partial x^2} + \frac{1}{2}\frac{\partial h}{\partial x}\frac{\partial h}{\partial x}\right]\right) = 0.$$

where the new conserved quantity, G is given by

$$G = hu - \frac{1}{2}\left(\frac{2}{3} + \beta_1\right)\frac{\partial}{\partial x}\left(h^3 \frac{\partial u}{\partial x}\right).$$

Using the appropriate substitution, we can recover the the conserved variable introduced by Clamond and Dutykh [3] for the rSWWE as well as for the Serre equations [].

Making this reformulation, we now have the equation of mass for the gSGN and an equation in conservation law form for G which is equivalent to the conservation of momentum equations as follows

$$\frac{\partial h}{\partial t} + \frac{\partial (uh)}{\partial x} = 0 \tag{6a}$$

$$\frac{\partial G}{\partial t} + \frac{\partial}{\partial x}\left(uG + \frac{gh^2}{2} - \frac{2}{3}\left(1 + \frac{3}{2}\beta_1\right) h^3 \frac{\partial u}{\partial x}\frac{\partial u}{\partial x} - \frac{1}{2}\beta_2 g h^2 \left[h\frac{\partial^2 h}{\partial x^2} + \frac{1}{2}\frac{\partial h}{\partial x}\frac{\partial h}{\partial x}\right]\right) = 0. \tag{6b}$$

with

$$G = uh - \frac{1}{3}\left(1 + \frac{3}{2}\beta_1\right)\frac{\partial}{\partial x}\left(h^3 \frac{\partial u}{\partial x}\right). \tag{6c}$$

This form of the equations and a bound on the wave speeds, allows us to solve (6) numerically using a combination of finite difference and finite volume methods as performed in [] for the SGN.

3. Numerical Method

The numerical method proposed for the gSGN, is very similar to methods published for the SGN []. For brevity, we will only provide a general overview of the method, whilst highlighting the important differences that need to be made to solve the gSGN over the SGN.

3.1. Overview

The numerical method for the gSGN equations proceeds very similarly to the SGN equations, we discretise space into cells of fixed width Δx, and used fixed time steps Δt. We then solved

in particular we have an elliptic equation which relates h, G and u and a set of conservation equations for h and G. To develop a numerical method for these equations we discretise space into cells of fixed width Δx, and used fixed time steps Δt. Using subscripts to denote spatial location, and superscripts to denote time

Following, [] we can therefore solve the gSGN equations using the following method

1. We begin with the cell averages $\bar{h}_j^n$ and $\bar{G}_j^n$ for all cells j
2. We solve (6c) using $\bar{h}_j^n$ and $\bar{G}_j^n$ to obtain an approximation to u_j^n for all cells j
3. We then solve (6a) and (6b) using a finite volume method with an approximate Riemann solver to obtain $\bar{h}_j^{n+1}$ and $\bar{G}_j^{n+1}$ at the next time step.

Since the finite volume solver is first-order accurate in time, we repeat these steps and do a convex combination to obtain a second-order accurate approximation to (6) in time.

3.2. Differences

- Just general form
- Highlight changes - limiters on gradients

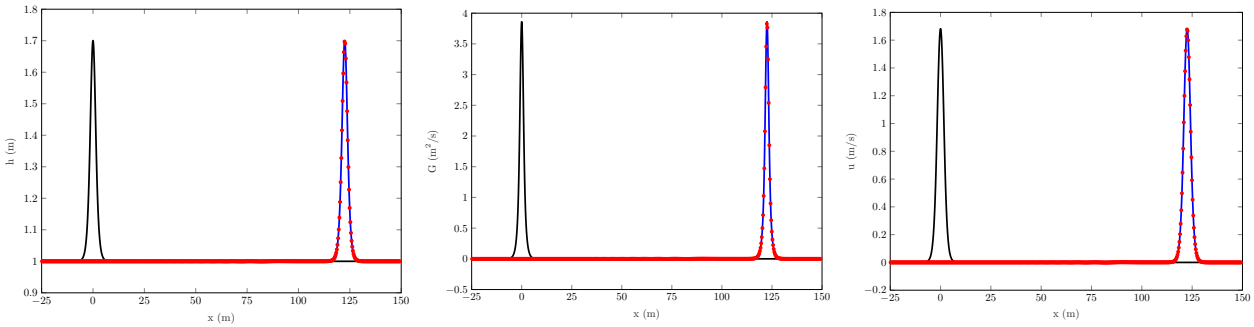

(a) h (b) G (c) u

Figure 2: Example plot comparing numerical for $t = 30s$. Initial (—), analytic solution (—), and numerical solution with $\Delta x \approx 0.06m$ (●) .

4. Validation

- Analytic solutions - we recover them (conservation and norm)
- Forced solutions - our numerical method can handle any combination of beta values, all terms are approximated with correct order of accuracy. Limiters on gradients off.

4.1. Analytic Solutions

4.1.1. Serre Equations ($\beta_1 = \beta_2 = 0$) - Solitary Travelling Wave Solution

When $\beta_1 = \beta_2 = 0$ the gSGN are equivalent to the SGN equations which admit the following travelling wave solution

$$h(x,t) = a_0 + a_1 \text{sech}^2\left(\kappa(x - ct)\right) \tag{7a}$$

$$u(x,t) = c\left(1 - \frac{a_0}{h(x,t)}\right) \tag{7b}$$

where

$$\kappa = \frac{\sqrt{3a_1}}{2a_0\sqrt{a_0 + a_1}} \tag{7c}$$

$$c = \sqrt{g\left(a_0 + a_1\right)} \tag{7d}$$

Results - Example,Convergence and Conservation Plot

4.1.2. SWWE ($\beta_1 = -\frac{2}{3}$ and $\beta_2 = 0$) - Dambreak Solution

$$h(x,0) = \begin{cases} h_0 & x < 0 \\ h_1 & x \geq 0 \end{cases} \tag{8}$$

$$u(x,0) = 0 \tag{9}$$

$$G(x,0) = 0 \tag{10}$$

We have an analytic solution for the SWWE for the discontinuous limit of these equations as $\alpha \to 0$. It is 3 constant states $(h_0, 0)$, (h_s, u_s) and $(h_1, 0)$ where

$$h_s = \frac{h_0}{2}\left[\sqrt{1 + 8\left(\frac{2h_s}{h_s - h_0}\left(\frac{\sqrt{gh_1} - \sqrt{gh_s}}{\sqrt{gh_0}}\right)\right)^2} - 1\right] \tag{11}$$

$$u_s = 2\left(\sqrt{gh_1} - \sqrt{gh_s}\right). \tag{12}$$

Where $(h_0, 0)$ and (h_s, u_s) are joined by a

Results - Example and Conservation Table

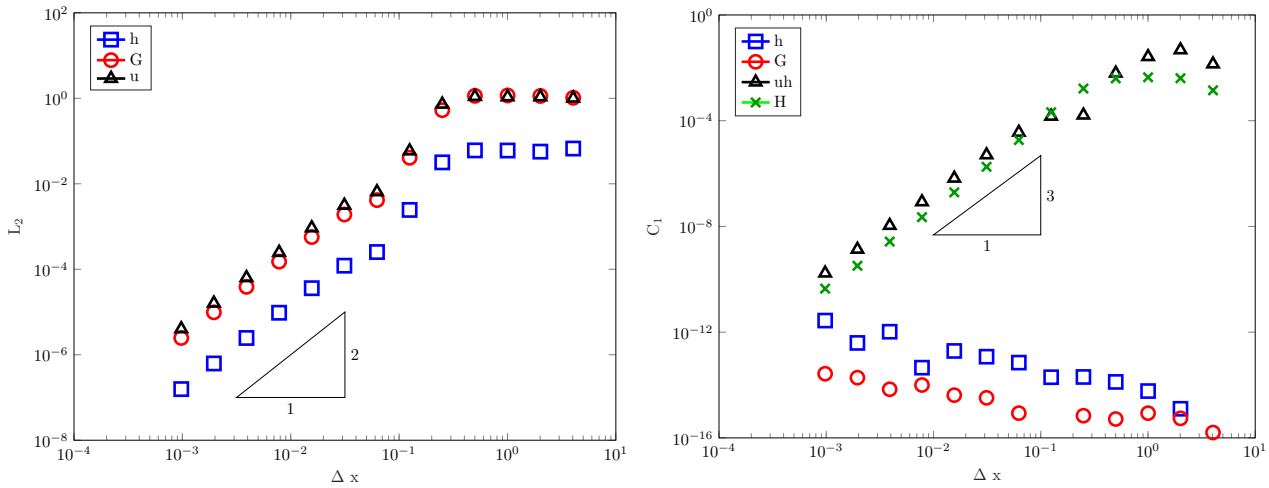

(a) L_2 (b) C_1, uh (Δ)

Figure 3: Convergence and Conservation Plots h (□) , G (○), u (Δ), $\mathcal{H}$ ×.

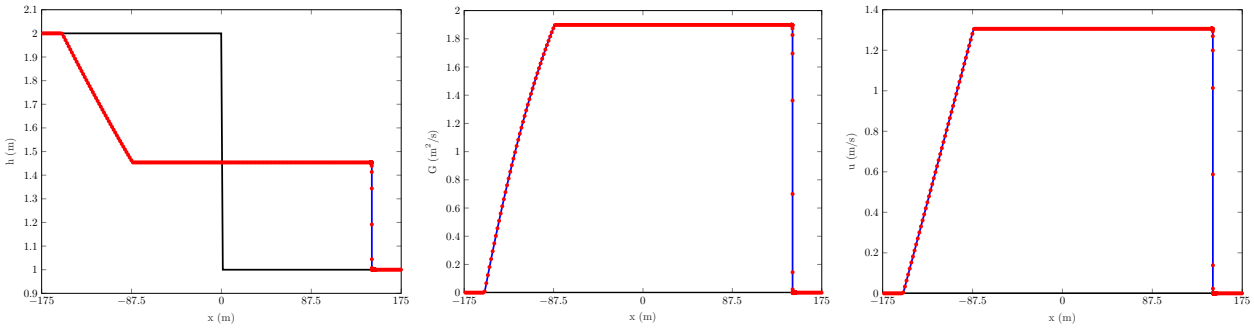

(a) h (b) G (c) u

Figure 4: Example plots for $t = 35s$. Initial (—), analytic solution (—), and numerical solution with $\Delta x \approx 0.03m$ (●) .

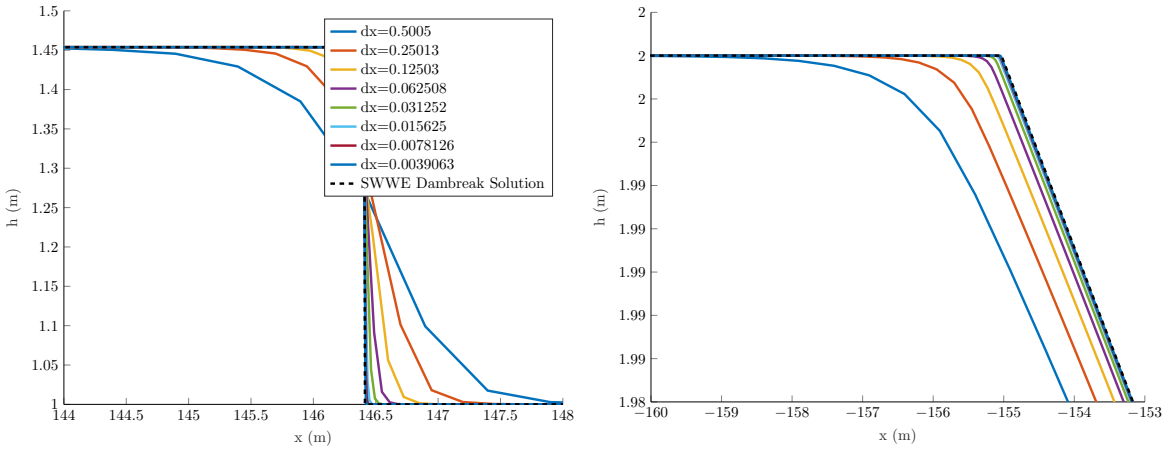

(a) h (b) h

Figure 5: Example plots for $t = 35s$. Initial (—), analytic solution (—), and numerical solution with $\Delta x \approx 0.03m$ (●) .

File Name: gSGNpaper.tex
Date: 28/06/2020 at 2:29pm

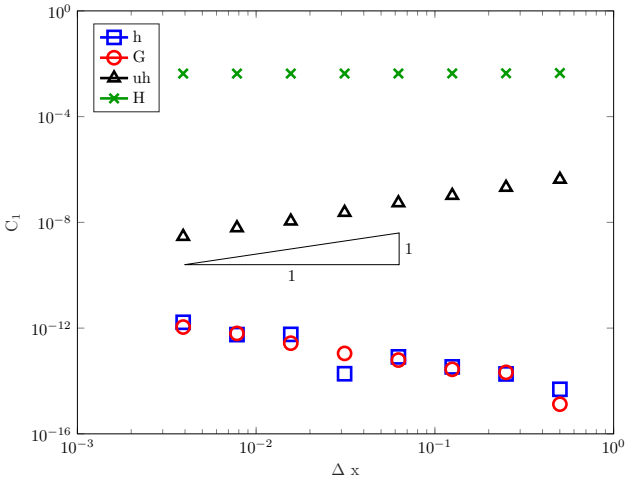

(a)

Figure 6: Conservation Plots h (□) , G (○), uh (△), $\mathcal{H}$ ×.

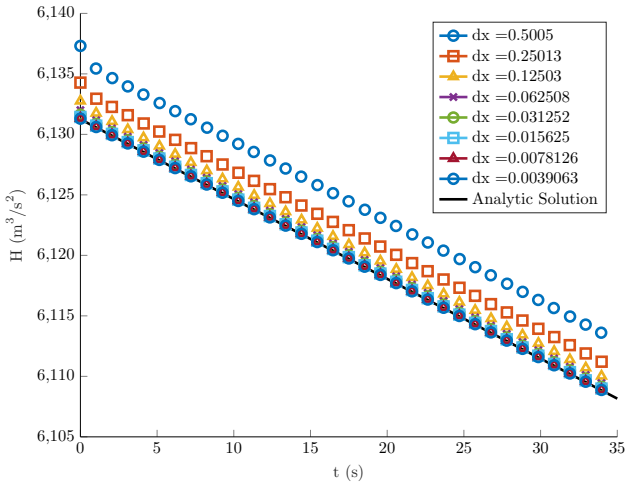

Figure 7: Plot of $\mathcal{H}$ over time.

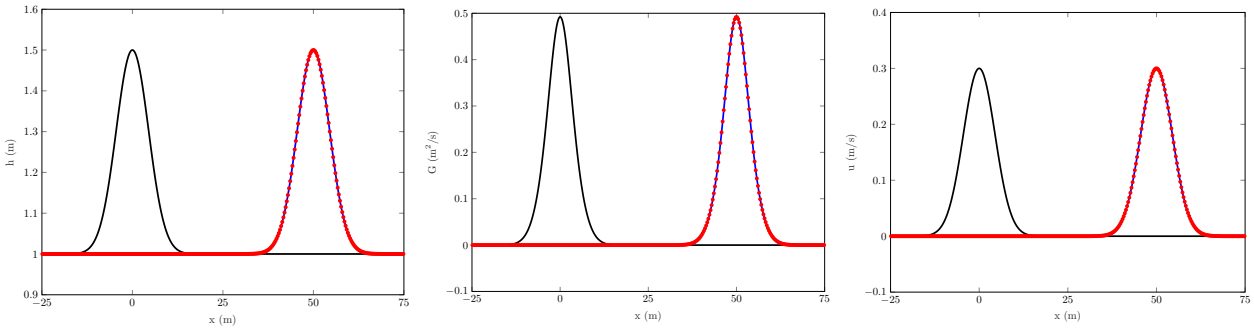

(a) h (b) G (c) u

Figure 8: Example plots Initial (—), analytic solution (—), and numerical solution with $\Delta x \approx 0.03m$ (●) .

4.2. Forced Solutions

To demonstrate the validity and versatility of our method to solve the gSGN whilst allowing varying β_i values, we make use of forced solutions. To generate a forced solution we consider the modified gSGN equations

$$\frac{\partial h}{\partial t} + \frac{\partial (uh)}{\partial x} = \frac{\partial h^*}{\partial t} + \frac{\partial (u^* h^*)}{\partial x} \tag{13a}$$

$$\begin{aligned} &\frac{\partial G}{\partial t} + \frac{\partial}{\partial x}\left(uG + \frac{gh^2}{2} - \frac{2}{3}\left(1 + \frac{3}{2}\beta_1\right) h^3 \frac{\partial u}{\partial x}\frac{\partial u}{\partial x} - \frac{1}{2}\beta_2 g h^2 \left[h\frac{\partial^2 h}{\partial x^2} + \frac{1}{2}\frac{\partial h}{\partial x}\frac{\partial h}{\partial x}\right]\right) = \\ &\frac{\partial G^*}{\partial t} + \frac{\partial}{\partial x}\left(u^* G^* + \frac{g\left(h^*\right)^2}{2} - \frac{2}{3}\left(1 + \frac{3}{2}\beta_1\right)\left(h^*\right)^3 \frac{\partial u^*}{\partial x}\frac{\partial u^*}{\partial x} - \frac{1}{2}\beta_2 g \left(h^*\right)^2 \left[h^*\frac{\partial^2 h^*}{\partial x^2} + \frac{1}{2}\frac{\partial h^*}{\partial x}\frac{\partial h^*}{\partial x}\right]\right) \end{aligned} \tag{13b}$$

which admit the solutions h^*, u^* and G^* assuming G^* appropriately satisfies (6c). Since these equations are satisfied for any chosen h^*, u^* and G^*, we can generated any desired solution. Since the left hand-side of these modified equations are approximated by our numerical method, if we combine the numerical method with analytic expressions for the right handside, we have a method that approximates the forced gSGN equation with the same convergence properties as the underlying numerical method for the gSGN equations.

Since we are free to choose h^*, u^* and G^* we can generate solutions and thus test our convergence properties for situations for which no analytic solution to the equations exist, in particular in this paper we are interested in solutions where the β values vary in space and time.

I have used this technique to investigate the method for the following forced solutions

$$h^*(x,t) = a_0 + a_1 \exp\left(\frac{(x - a_2 t)^2}{2a_3}\right) \tag{14a}$$

$$u^*(x,t) = a_4 \exp\left(\frac{(x - a_2 t)^2}{2a_3}\right) \tag{14b}$$

$$\beta_1(x,t) = a_6 \tag{14c}$$

$$\beta_2(x,t) = a_7 \tag{14d}$$

where G^* is determined by (6c) with the above values.

Results - Example plot and L1 convergence, comment that this worked for all beta values, and we only show one for conciseness

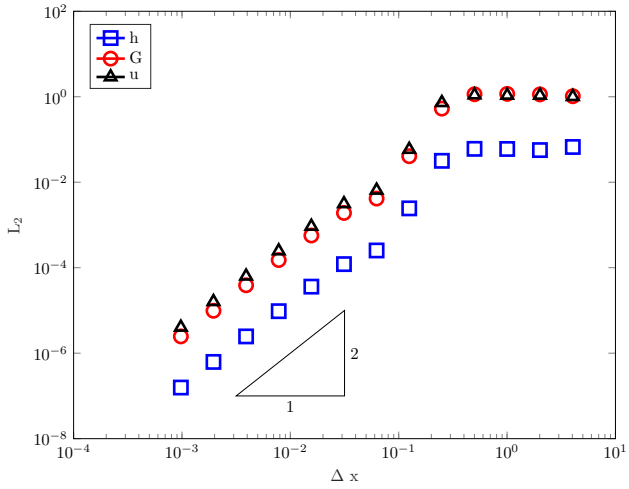

(a) L_2

Figure 9: Convergence and Conservation Plots h (□) , G (○), u (△).

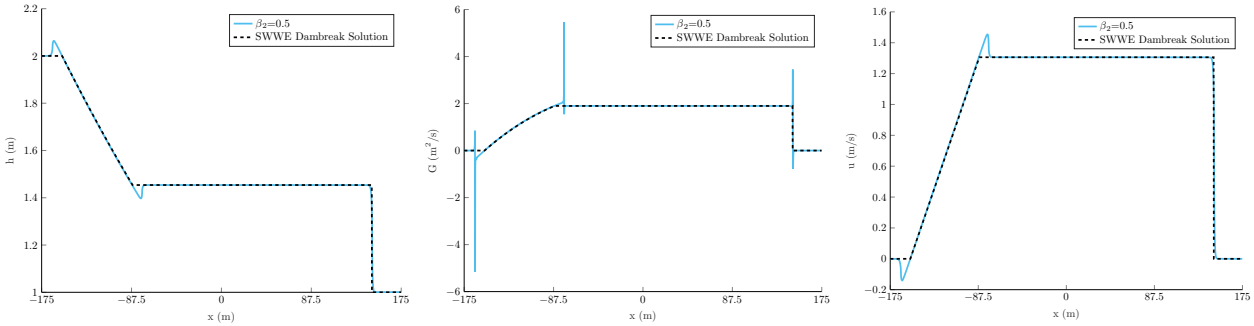

(a) h (b) G (c) u

Figure 10: Plot of example numerical solution for representative memeber of regularised SWWE family to smooth dambreak problem at $t = 35s$.

5. Smooth Dambreak Study

$$h(x,0) = h_0 + \frac{h_1 - h_0}{2}\left(1 + \tanh\left(\frac{x}{\alpha}\right)\right) \tag{15}$$

$$u(x,0) = 0 \tag{16}$$

$$G(x,0) = 0 \tag{17}$$

5.1. Regularised SWWE Family $\beta_2 = \frac{2}{3} + \beta_1$

Justify interest, cite denys paper on regularised SWWE

- we do get nice well behaved transitions between behaviours when varying β values we get nice convergence.
- Although solutions look nice in h, in G there can be quite large values in the smoothed regions. However, u still looks quite nice.

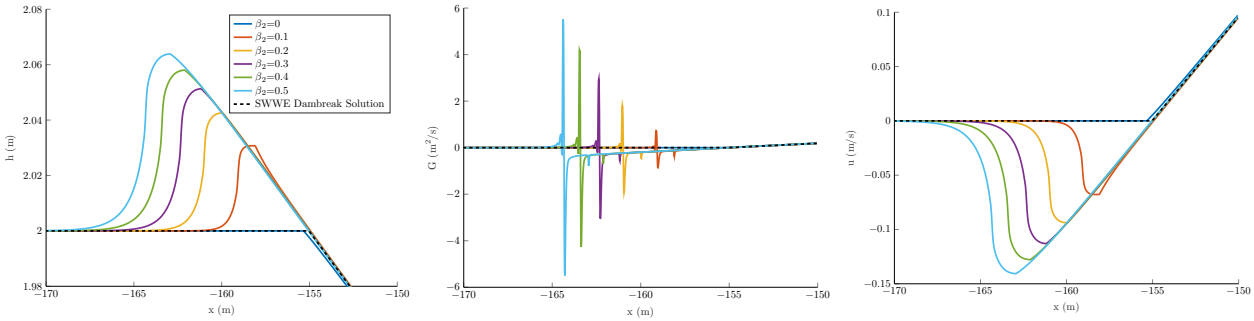

(a) h top of rarefaction fan (b) G top of rarefaction fan (c) u top of rarefaction fan

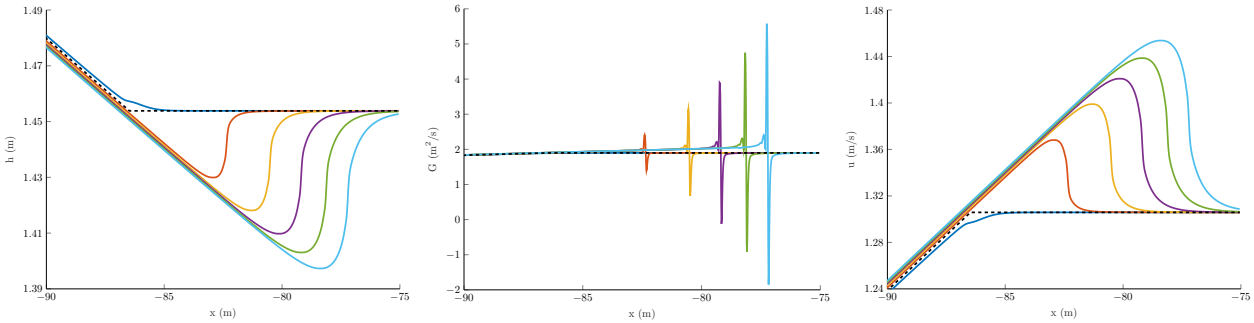

(d) h bottom of rarefaction fan (e) G bottom of rarefaction fan (f) u bottom of rarefaction fan

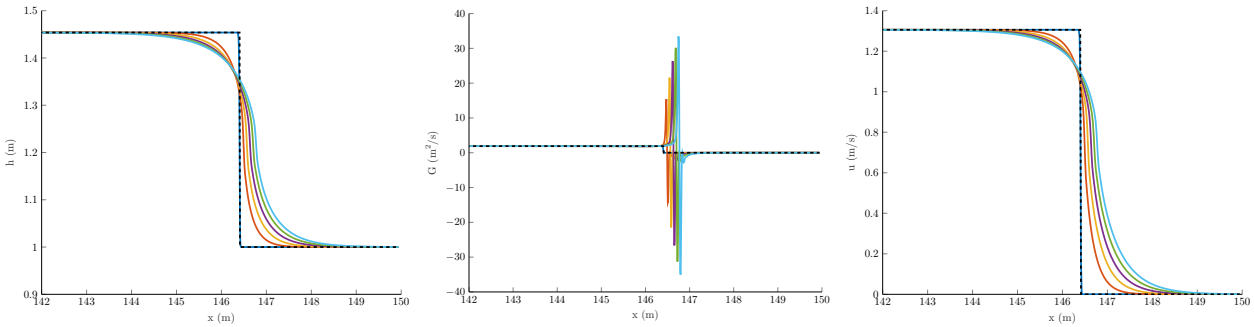

(g) h shock front (h) G shock front (i) u shock front

Figure 11: Plot of multiple smooth dambreak numerical solutions at $t = 35s$. $\beta_2 = 0$ (—), $\beta_2 = 0.1$ (—), $\beta_2 = 0.2$ (—), $\beta_2 = 0.3$ (—), $\beta_2 = 0.4$ (—), $\beta_2 = 0.5$ (—).

Colour region	Condition
first blue	$\frac{x}{t} \leq u_s - \sqrt{gh_s}$
first red	$u_s - \sqrt{gh_s} \leq \frac{x}{t} \leq u_s - \sqrt{gh_s}\sqrt{\frac{\beta_2}{\frac{2}{3}+\beta_1}}$
first green	$u_s - \sqrt{gh_s}\sqrt{\frac{\beta_2}{\frac{2}{3}+\beta_1}} \leq \frac{x}{t} \leq u_s$
second green	$u_s \leq \frac{x}{t} \leq u_s + \sqrt{gh_s}\sqrt{\frac{\beta_2}{\frac{2}{3}+\beta_1}}$
second red	$u_s + \sqrt{gh_s}\sqrt{\frac{\beta_2}{\frac{2}{3}+\beta_1}} \leq \frac{x}{t} \leq u_s + \sqrt{gh_s}$
second blue	$u_s + \sqrt{gh_s} \leq \frac{x}{t}$

Table 2: Regions for plots.

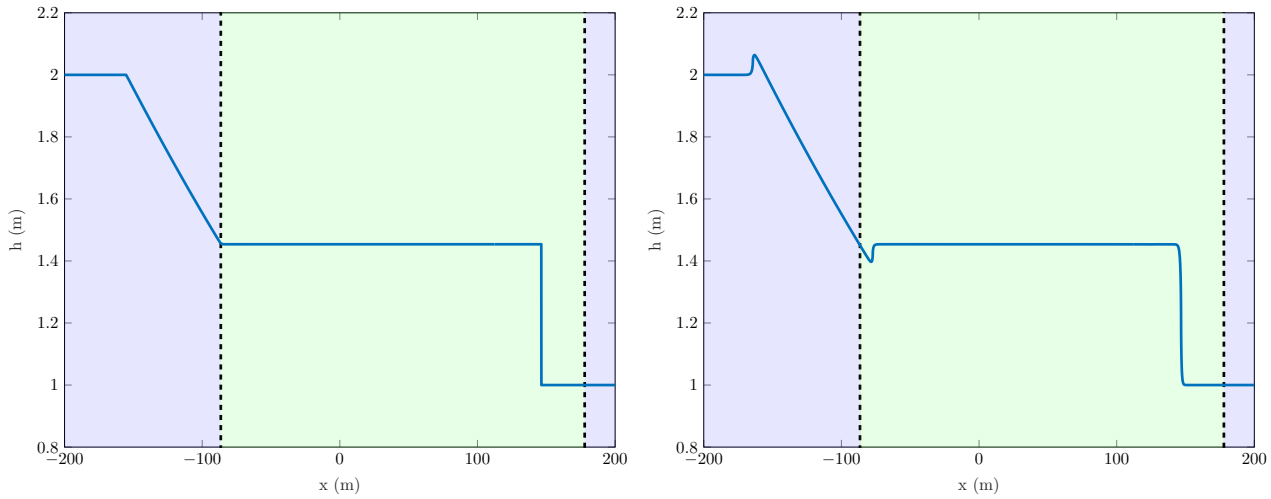

(a) $\beta_2 = 0$ (b) $\beta_2 = 0.5$

Figure 12: Regions of wave speeds for the smooth dambreak numerical solution at $t = 35s$.

β_2	h	G	uh	$\mathcal{H}$
0	5.8×10^{-13}	6.3×10^{-13}	6.3×10^{-9}	3.7×10^{-3}
0.1	6.4×10^{-13}	6.4×10^{-13}	9.8×10^{-6}	3.9×10^{-3}
0.2	6.7×10^{-13}	6.4×10^{-13}	1.1×10^{-5}	4.1×10^{-3}
0.3	6.9×10^{-13}	6.4×10^{-13}	1.2×10^{-5}	4.3×10^{-3}
0.4	7.1×10^{-13}	6.6×10^{-13}	1.2×10^{-5}	4.4×10^{-3}
0.5	7.1×10^{-13}	6.5×10^{-13}	1.3×10^{-5}	4.6×10^{-3}

Table 3: Conservation errors for Regularised SWWE for the solutions provided above with $\beta_1 = \beta_2 - \frac{2}{3}$.

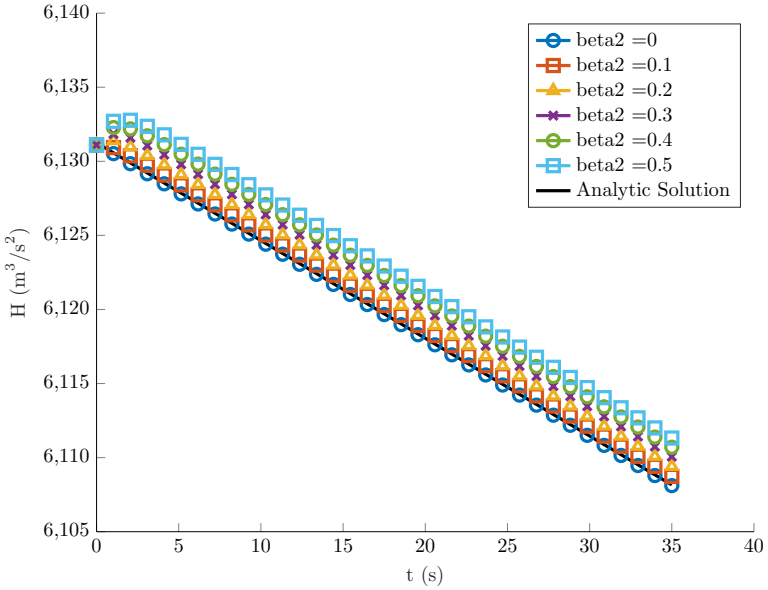

Figure 13: Energy over time for the numerical solutions, for the β values in the Regularised SWWE family.

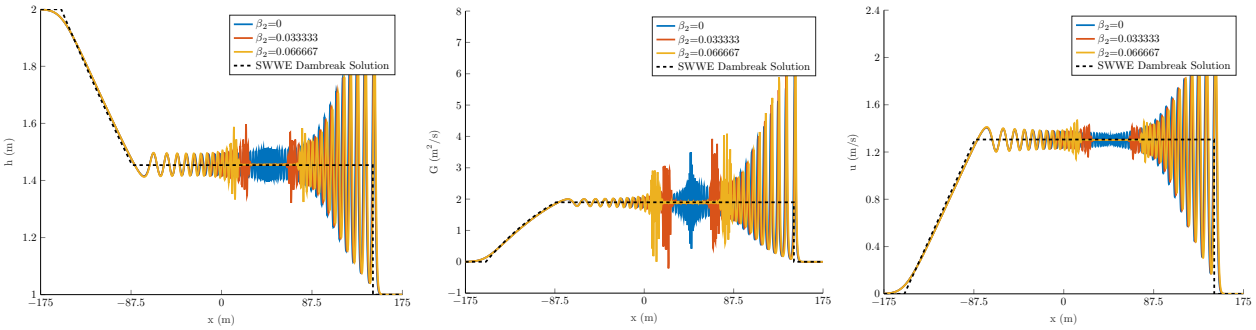

(a) h (b) G (c) u

Figure 14: Plot of multiple smooth dambreak numerical solutions at $t = 35s$.

β_1	h	G	uh	$\mathcal{H}$
0	8.0×10^{-13}	6.3×10^{-13}	3.3×10^{-7}	3.8×10^{-6}
$\frac{1}{30}$	8.1×10^{-13}	6.4×10^{-13}	3.5×10^{-7}	1.9×10^{-5}
$\frac{1}{15}$	8.2×10^{-13}	6.3×10^{-13}	5.8×10^{-7}	1.1×10^{-4}

Table 4: Conservation errors for Modified Dispersion Serre Equations for the solutions provided above with $\beta_2 = \beta_1$.

5.2. Modified Dispersion Serre Family $\beta_2 = \beta_1$

Justify interest, cite denys paper on dispersion modified equations
Points:

- we do get nice well behaved transitions between behaviours when varying β
- Dispersive wave train location well approximated by using the linear wave speeds. Although the bump around these bounds suggests non-linear effects are important as well, particularly close to transitions across the wavespeed boundaries.
- Improved dispersion may better approximate the dispsersion relation when $k \ll 1$, but at the cost of the middle of the dispersive wave train
- We get the bump behaviour observed in the db paper, but now dispersive wave trains are separate.
- Conservation is pretty similar, except for energy where it gets worse - this suggests that we will need finer grids to get good solutions particularly when gradients are large.

5.3. Serre To SWWE Family $\beta_2 = 0$ and $-\frac{2}{3} \leq \beta_1 \leq 0$

Justify interest, switching dispersion on and off, effect and giving structure/understanding to various schemes that turn it on and off.
Points:

- we do get convergence, but most of the convergent behaviour occurs very close to the critical SWWE value. This is because gradients are large in the initial conditions
- Middle of dispersive wave train, and base and top of rarefaction fan most affected (closer to Serre)
- Still quite a large dispersive wave train even for β_1 values close to $-2/3$. (This appears to justify switching)
- the front of the shock became larger for some intermediate values.

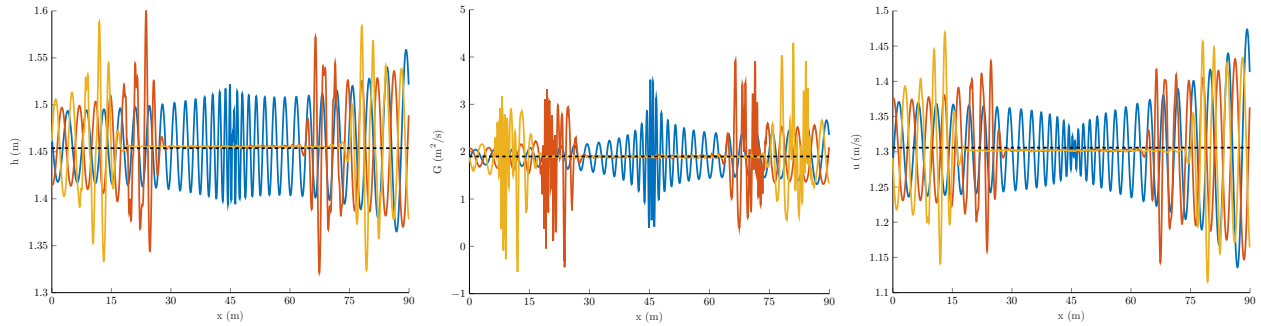

(a) h in middle of dispersive wave train (b) G in middle of dispersive wave train (c) u in middle of dispersive wave train

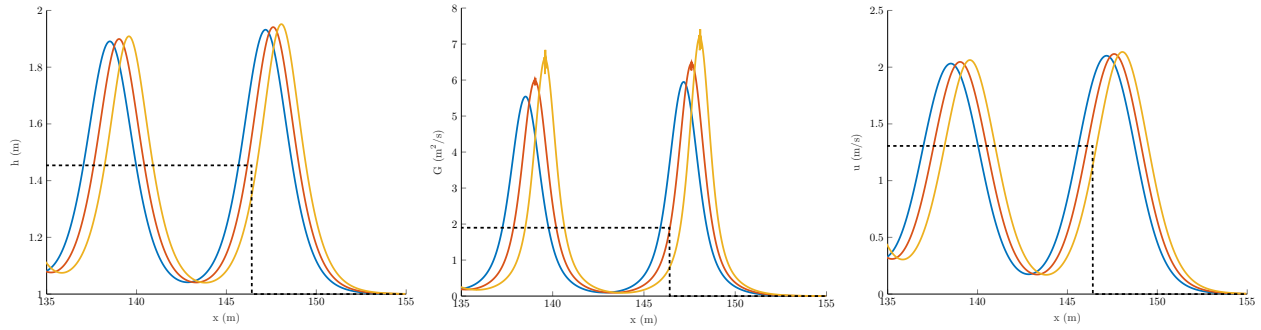

(d) h Front of dispersive wave train (e) G Front of dispersive wave train (f) u Front of dispersive wave train

Figure 15: Plot of multiple smooth dambreak numerical solutions at important locations at $t = 35s$.

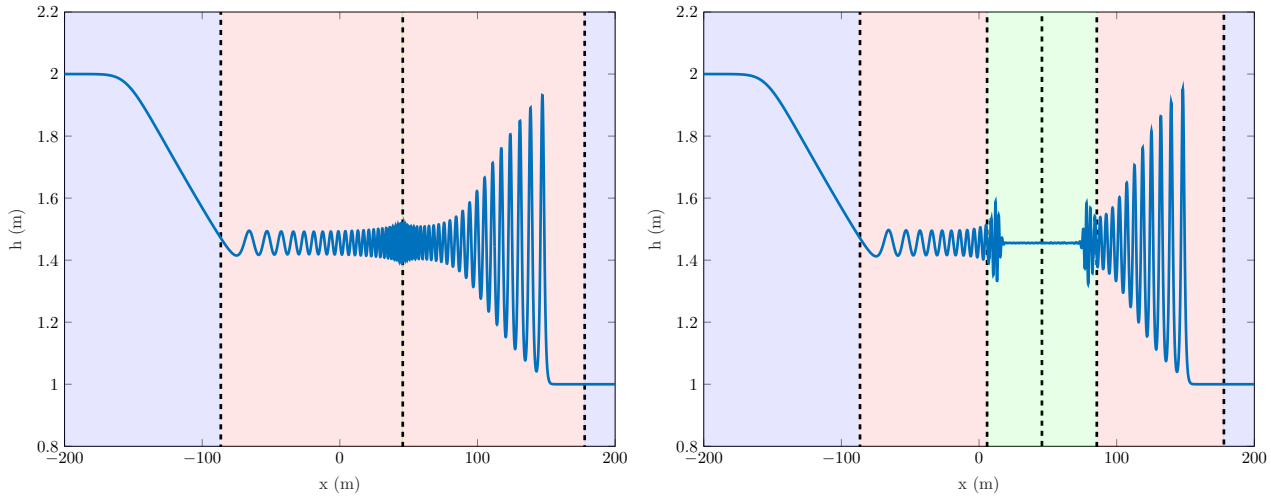

(a) $\beta_1 = \beta_2 = 0$ (b) $\beta_1 = \beta_2 = \frac{1}{15}$

Figure 16: Regions of wave speeds for the smooth dambreak numerical solution at $t = 35s$.

File Name: gSGNpaper.bbl
Date: 28/06/2020 at 2:29pm

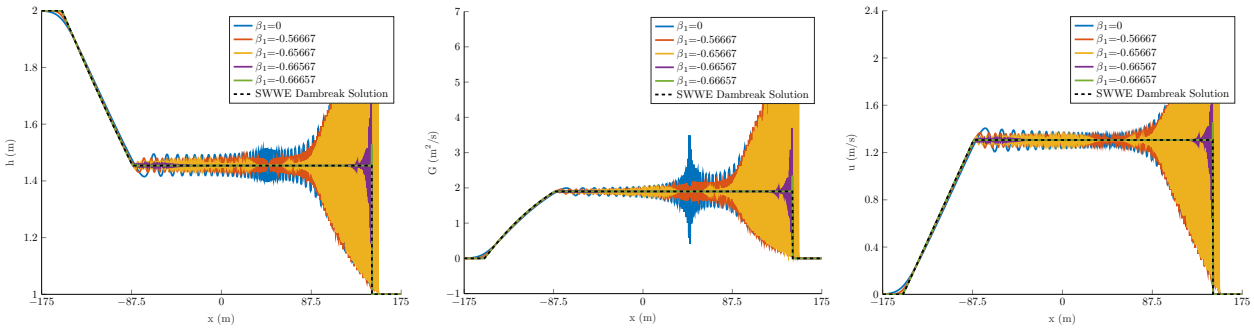

(a) h (b) G (c) u

Figure 17: Plot of multiple smooth dambreak numerical solutions at $t = 35s$.

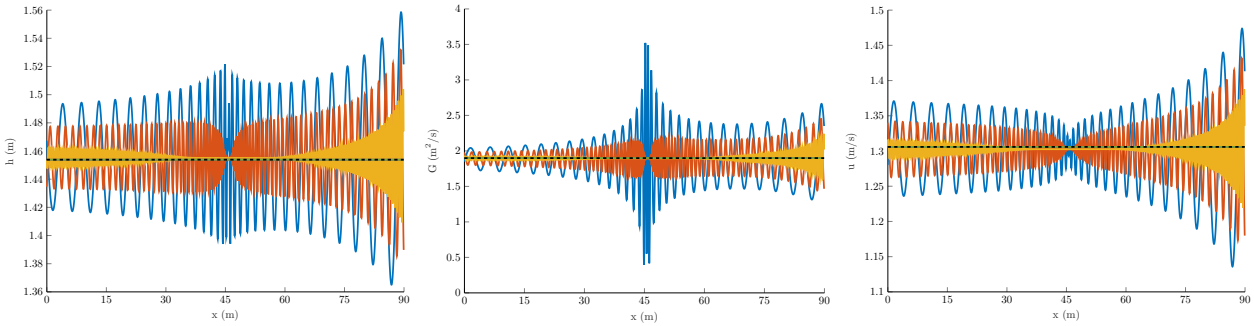

(a) h middle of dispersive wave train (b) G middle of dispersive wave train (c) u middle of dispersive wave train

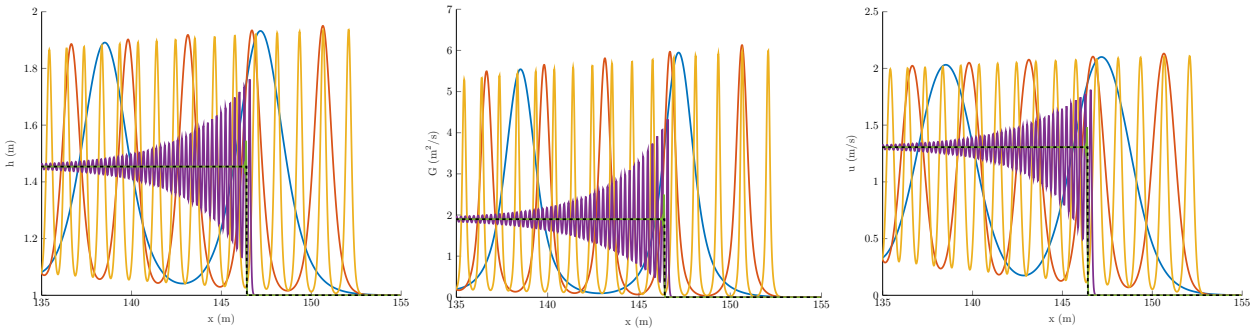

(d) h front of dispersive wave train (e) G front of dispersive wave train (f) u front of dispersive wave train

Figure 18: Plot of multiple smooth dambreak numerical solutions at $t = 35s$.

β_1	h	G	uh	$\mathcal{H}$
0	8.0×10^{-13}	6.3×10^{-13}	3.3×10^{-7}	3.8×10^{-6}
$-\frac{2}{3} + 10^{-1}$	7.2×10^{-13}	6.3×10^{-13}	3.0×10^{-6}	6.3×10^{-6}
$-\frac{2}{3} + 10^{-2}$	6.6×10^{-13}	6.2×10^{-13}	3.2×10^{-5}	3.7×10^{-4}
$-\frac{2}{3} + 10^{-3}$	6.0×10^{-13}	6.3×10^{-13}	1.2×10^{-5}	3.7×10^{-3}
$-\frac{2}{3} + 10^{-4}$	5.9×10^{-13}	6.2×10^{-13}	1.2×10^{-6}	3.7×10^{-3}

Table 5: Conservation errors for Serre To SWWE Faimly of Equations for the solutions provided above with $\beta_2 = 0$ and $-\frac{2}{3} \leq \beta_1 \leq 0$.

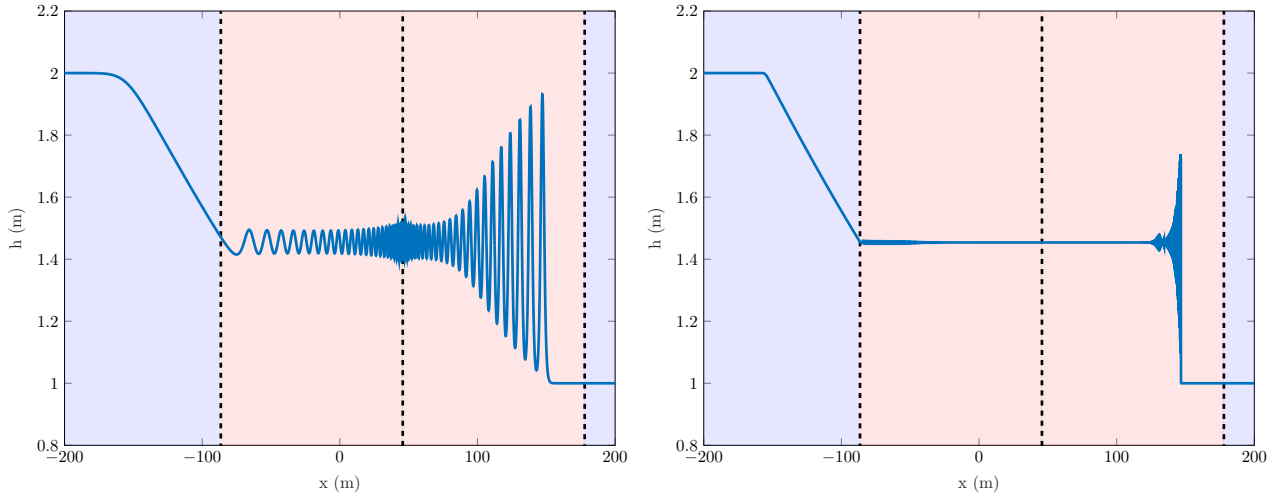

(a) $\beta_1 = \beta_2 = 0$

(b) $\beta_1 = -\frac{2}{3} + 10^{-3}$ and $\beta_2 = 0$

Figure 19: Regions of wave speeds for the smooth dambreak numerical solution at $t = 35s$.

- Trade-off between momentum convergence (since G = uh for SWWE) and energy convergence. Dispersive models conserve energy better due to smooth solutions, but conserve momentum worse because conserved quantitiy is not uh.

[1] D. Lannes and P. Bonneton. Derivation of asymptotic two-dimensional time-dependent equations for surface water wave propagation. *Physics of Fluids*, 21(1):16601, 2009.

[2] D. Clamond, D. Dutykh, and D. Mitsotakis. Conservative modified Serre-Green-Naghdi equations with improved dispersion characteristics. *Communications in Nonlinear Science and Numerical Simulation*, 45, 2017.

[3] D. Clamond and D. Dutykh. Non-dispersive conservative regularisation of nonlinear shallow water (and isentropic euler equations). *Communications in Nonlinear Science and Numerical Simulation*, 55, 2018.